IEEE Access
Multidisciplinary ⋮ Rapid Review ⋮ Open Access Journal

Received August 17, 2020, accepted September 7, 2020, date of publication September 15, 2020, date of current version October 7, 2020.

Digital Object Identifier 10.1109/ACCESS.2020.3024195

Analysis and Implementation of Constrained MTPA Criterion for Induction Machine Drives

ZHIHUA PENG
School of Electrical Engineering, Shaoyang University, Shaoyang 422000, China
e-mail: 304151342@qq.com

This work was supported by the Research Foundation of Education Bureau of Hunan Province, China, under Grant 18C0828.

ABSTRACT Maximum torque per amper (MTPA) control can realize the minimum copper loss control of induction motor, which is often applied below the rated speed. In this paper, MTPA control is firstly extended from the constant torque mode to the constant apparent power mode and the constant voltage mode, and realizes MTPA control of induction motor in the whole speed range. Firstly, this paper establishes a MTPA-based nonlinear optimization problem in the whole speed range. Then, this optimization problem is analyzed and the analytical expressions are obtained for three different modes. Finally, finite control set-model predictive current control is adopted in this paper to achieve the fast stator current tracking. In the experimental part, the proposed algorithm is compared with the classical control strategy in this paper. The experimental results show that for the light load, the proposed algorithm reduces the stator current magnitude and improves the efficiency of induction machines.

INDEX TERMS Induction machine, constrained MTPA criterion, predictive control.

I. INTRODUCTION

In the control strategy of AC motor, the maximum torque per ampere (MTPA) control strategy is often used to achieve the optimal control of excitation current and torque current and improve the system efficiency [1]–[5]. Limited by maximum stator current magnitude and maximum stator voltage, induction motors usually operates in constant torque mode below the rated speed and in constant apparent power mode above the rated speed, that is, field weakening mode [6], [7]. In constant torque mode, induction motors usually adopt the rated excitation, that is, the rotor flux amplitude keeps constant [8], [9]. In the constant apparent power mode, the limit of bus voltage must be satisfied by reducing the rotor flux amplitude [10]–[12]. At present, the research of field-weakening control mainly focuses on how to achieve the maximum torque control in the field-weakening mode at voltage and current limits [13]–[16]. There are three kinds of field-weakening control algorithms for induction motors. Firstly, the excitation current is inversely proportional to the rotor speed in the field weakening mode. This kind of algorithm is simple, but it can not achieve optimal control according to the load torque [17]. The second method is based on the accurate motor model. This method can theoretically obtain the maximum torque control, but it is difficult to apply in practice because of its strong parameter dependence and complex calculation [18]. The third method is to generate excitation current based on voltage controller. This method can achieve high steady-state torque output capability, independent of motor parameters, but the voltage controller increases the complexity of the system [19]. Reference [20] compares four methods of field weakening, and analyses the advantages and disadvantages of different methods. These four control schemes fully utilize the maximum available voltage and current and can produce the maximum possible torque in the entire field-weakening region. Reference [21] applies model predictive control to the field weakening control, which enhances the robustness of the system. In [22], MTPA is utilized to compute excitation current and torque current references for induction machines, but this paper can not extend MTPA to field weakening mode. In [23], the MTPA control based on the measured current-torque curve is proposed, which does not depend on the parameters of induction machines and improve the robustness of the system.

In this paper, the MTPA control strategy is extended to the field weakening mode. Firstly, the MTPA-based optimization problem in the whole speed region is established. Then the analytical expressions of the optimization problem are given in constant torque mode, constant apparent power mode and constant voltage mode, which can obtain

The associate editor coordinating the review of this manuscript and approving it for publication was Ton Duc Do.

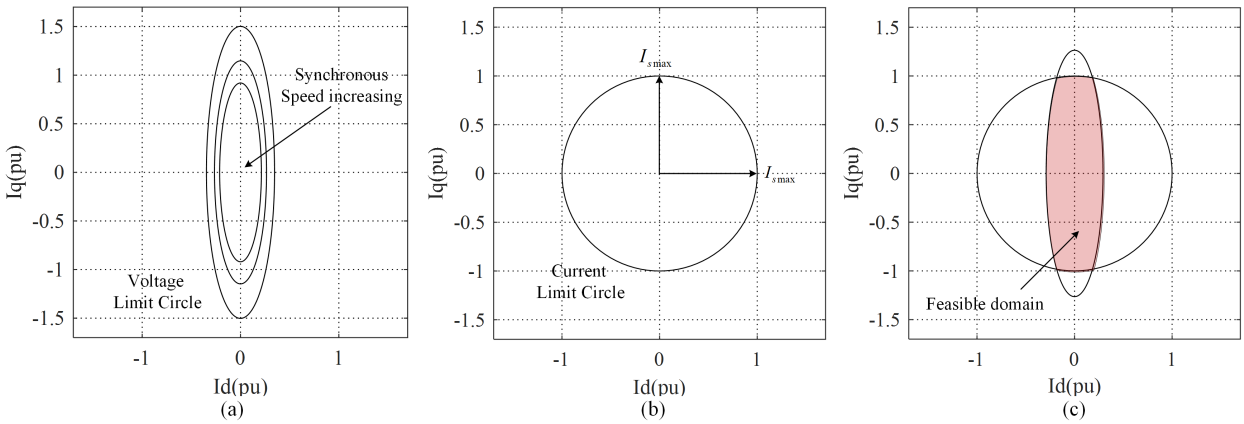

FIGURE 1. The feasible domain at voltage and current limits. (a) Voltage constraint, (b) Current constraint, (c) The feasible domain at voltage and current limits.

the excitation current and torque current references. Finally, predictive current control is applied to track the stator current references.

The arrangement of this paper is as follows. In Section II, the mathematical model of induction motor and the constraints of voltage and current are introduced. Section III introduces the optimization problem based on maximum torque control and the analytical expressions in constant torque mode, constant apparent power mode and constant voltage mode. Section IV analyses the constrained MTPA criterion for induction machines, and then achieves the analytic expressions in three modes. In Section V, the algorithm proposed in this paper is experimentally studied. Section VI summarizes this paper.

II. MATHEMATICAL MODEL OF INDUCTION MACHINE AND VSI

In the $d-q$ reference frame system with arbitrary rotation speed ω, the mathematical equations of induction motor is shown as (1)-(3), where $\psi_s^\omega = L_s i_s^\omega + L_m i_r^\omega$, $\psi_r^\omega = L_m i_s^\omega + L_r i_r^\omega$ [24], [25].

$$v_s^\omega = R_s i_s^\omega + \frac{d\psi_s^\omega}{dt} + jw\psi_s^\omega \tag{1}$$

$$0 = R_r i_r^\omega + \frac{d\psi_r^\omega}{dt} + j(\omega - \omega_r)\psi_r^\omega \tag{2}$$

$$T_e = \frac{3}{2}P\frac{L_m}{L_r} Im\left\{\overline{\psi_r^\omega} i_s^\omega\right\} \tag{3}$$

When the d-axis of the rotation reference frame coincides with the direction of the rotor flux vector, stator current vector can be expressed as an equation (4), where i_{ds}^e and i_{qs}^e are the d-axis component and d-axis component, respectively. the d-axis component of the rotor flux vector, ψ_{qr}^e, is zero, that is, $\psi_{qr}^e = 0$. The ψ_{dr}^e can be expressed as an equation (5), where i_{ds}^e is the excitation current. In the steady state of induction motor, the electromagnetic torque can be simplified to equation (6), where p denotes pole pairs of induction motor.

$$i_s^e = i_{ds}^e + j i_{qs}^e \tag{4}$$

$$\psi_{dr} = \frac{L_m}{1 + p\left(L_r/R_r\right)} i_{ds} \tag{5}$$

$$T_e = \frac{3}{2}p\frac{L_m^2}{L_r} I_{ds}^e I_{qs}^e \tag{6}$$

In the operation of induction motor, the excitation current and the torque current of induction motor must also satisfy both the voltage limit circle and the current limit circle. The equations of voltage limit circle and current limit circle are respectively shown in equations (7) and (8), where V_{smax} is the maximum stator voltage of induction motor and $\sigma = 1 - \left(\frac{L_m^2}{L_s L_r}\right)$ [26]. The graphical representation is shown in Fig.1.

$$\left(\omega_e \sigma L_s I_{qs}^e\right)^2 + \left(\omega_e L_s I_{ds}^e\right)^2 \le V_{s\max}^2 \tag{7}$$

$$\left(I_{ds}^e\right)^2 + \left(I_{qs}^e\right)^2 \le I_{s\max}^2 \tag{8}$$

III. FIELD WEAKENING STRATEGY BASED ON MAXIMUM TORQUE CONTROL

The basic principle of field weakening control based on maximum torque control is to calculate the reference values of stator excitation current and stator torque current at voltage and current limits to achieve maximum torque control. Then, the predictive current control is used to track the reference values of stator excitation current and stator torque current quickly.

In the steady state of induction motor, the electromagnetic torque T_e can be expressed as the equation (9). The maximum torque control of induction motors at voltage and current limits can be described as an optimization problem, as shown in equation (9)-(11). In the later part of this paper, for convenience, the superscript of I_{ds}^e is omitted and denoted as I_{ds}.

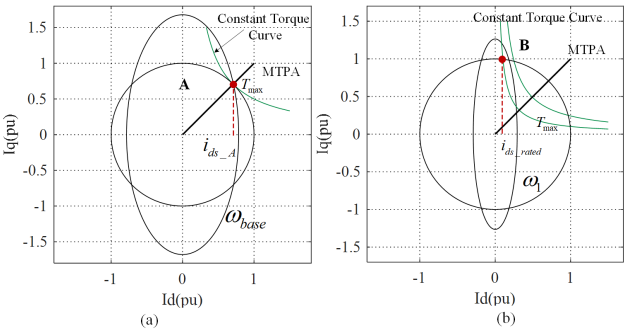

FIGURE 2. The diagram of the synchronous speed ω_{base}, ω_1 calculation.

So is I_{qs}^e.

$$max\ T_e = \frac{3}{2}p\frac{L_m^2}{L_r}I_{ds}^e I_{qs}^e \tag{9}$$

$$s.t.\ \left(\omega_e\sigma L_s I_{qs}^e\right)^2 + \left(\omega_e L_s I_{ds}^e\right)^2 \le V_{s\max}^2 \tag{10}$$

$$\left(I_{ds}^e\right)^2 + \left(I_{qs}^e\right)^2 \le I_{s\max}^2 \tag{11}$$

The optimization problem (9)-(11) is a constrained nonlinear programming problem, and it is usually difficult to find an analytical expression. However, the optimization problem (9)-(11) can be decomposed into several subproblems, each of which can be solved by the characteristic curves of induction motors, such as MTPA curve, constant torque curve and voltage limit circle. In this paper, the analytical expressions of the above optimization problems are composed of three parts, respectively in constant torque mode, constant apparent power mode and constant voltage mode. Three modes are divided according to the synchronous speed ω_e of induction motor, where ω_e is the angular frequency of the supply voltage at steady state, and not the rotational angular speed of the rotor. The intersection point of the current limit circle and the MTPA curve of the induction motor is marked as point A, as shown in Fig.2. With the increase of the synchronous speed ω_e of induction motor, the voltage limit circle is shrinking. When the voltage limit circle is reduced to the circle passing through point A, the synchronous tachometer of the induction motor is denoted as ω_{base}, as shown in Fig.2 (a), where the excitation current corresponding to point A is denoted as I_{ds_A}. By combining three equations (12)-(14), the equation of ω_{base} can be obtained. Therefore, in the constant torque mode, the range of ω_e is $0 < \omega_e \le \omega_{base}$.

$$\left(\omega_{base}\sigma L_s I_{ds\_A}\right)^2 + \left(\omega_{base} L_s I_{qs\_A}\right)^2 = V_{s\max}^2 \tag{12}$$

$$\left(I_{ds\_A}\right)^2 + \left(I_{qs\_A}\right)^2 = I_{s\max}^2 \tag{13}$$

$$I_{ds\_A} = I_{qs\_A} \tag{14}$$

$$\omega_{base} = \frac{V_{s\max}}{\sqrt{I_{ds\_A}^2\left(L_s^2 - \sigma^2 L_s^2\right) + \left(\sigma L_s I_{s\max}\right)^2}} \tag{15}$$

When $\omega_e > \omega_{base}$, the voltage limit circle decreases with the increase of the synchronous speed ω_e of induction motor. When there is only one intersection point between the voltage limit circle and current limit circle, the synchronous speed of induction motor is denoted as ω_1 and this intersection point is denoted as point B, as shown in Fig.2 (b). At this time, the excitation current corresponding to point B is zero, i.e. $I_{ds\_B} = 0$. By combining the equations (16)-(18), the expression of the synchronous speed ω_1 can be obtained, as shown in equation (19). In the constant apparent power mode, the range of ω_e is $\omega_{base} < \omega_e \le \omega_1$. In the constant voltage mode, the range of ω_e is $\omega_1 < \omega_e$.

$$\left(\omega_1\sigma L_s I_{ds\_B}\right)^2 + \left(\omega_1 L_s I_{qs\_B}\right)^2 = V_{s\max}^2 \tag{16}$$

$$\left(I_{ds\_B}\right)^2 + \left(I_{qs\_B}\right)^2 = I_{s\max}^2 \tag{17}$$

$$I_{ds\_B} = 0 \tag{18}$$

$$\omega_1 = \left(V_{s\max}/I_{s\max}\right)\sqrt{\left(L_s^2 + \sigma^2 L_s^2\right)/\left(2L_s^4\sigma^2\right)} \tag{19}$$

In order to solve the nonlinear optimization problem (9)-(11), this paper elaborates the equations of the optimal excitation current and the torque current in the constant torque mode, the constant apparent power mode and the constant voltage mode, respectively. The diagram of the solutions is shown in Fig.3.

1) THE CONSTANT TORQUE MODE ($0 < \omega_e \le \omega_{base}$)

In the constant torque mode, the diagram of the voltage limit circle and the current limit circle is shown in Fig.3 (a). When the induction motor operates at the intersection point A of the MTPA curve and the current limit circle, the induction motor can output the maximum torque. Therefore, the excitation current I_{ds_A} and the torque current I_{qs_A} corresponding to the point A can be calculated by the equation (20). The maximum electromagnetic torque $T_{\max}$ can be expressed as the equation (21).

$$I_{ds\_A} = I_{qs\_A} = \sqrt{I_{s\max}^2/2} \tag{20}$$

$$T_{\max} = \frac{3}{2}p\frac{L_m^2}{L_r}I_{ds\_A}\sqrt{I_{s\max}^2 - \left(I_{ds\_A}\right)^2} \tag{21}$$

2) THE CONSTANT APPARENT POWER MODE ($\omega_{base} < \omega_e \le \omega_1$)

In the constant apparent power mode, the diagram is shown in Fig.3 (b). When the excitation current and the torque current operates at the intersection point B of the voltage limit circle and the current limit circle, the induction motor can output the maximum torque.

$$\left(\omega_e\sigma L_s I_{ds\_B}\right)^2 + \left(\omega_e L_s I_{qs\_B}\right)^2 = V_{s\max}^2 \tag{22}$$

$$\left(I_{ds\_B}\right)^2 + \left(I_{qs\_B}\right)^2 = I_{s\max}^2 \tag{23}$$

The excitation current and the torque current at point B can be obtained by solving the equations (22)-(23), respectively, as shown in the equations (24) and (25), so the maximum output torque of the induction motor is expressed in the

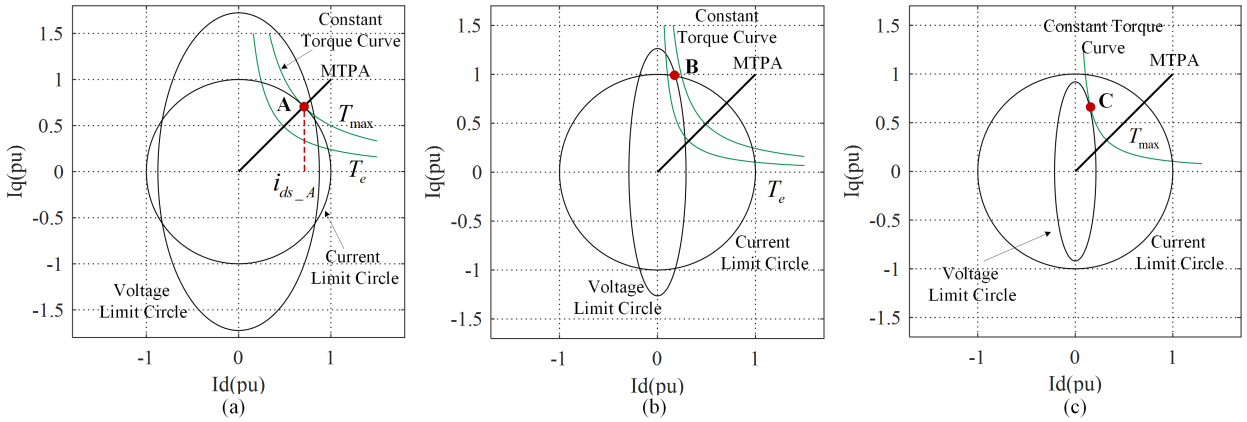

FIGURE 3. The diagram of optimal stator currents of field weakening based on maximum torque control (a)the constant torque mode (b)the constant apparent power mode (c)the constant voltage mode.

equation (26).

$$I_{ds\_B} = \frac{\sqrt{\left(V_{s\max}/\omega_e\right)^2 - \left(\sigma L_s I_{s\max}\right)^2}}{\sqrt{L_s^2 - \left(\sigma L_s\right)^2}} \tag{24}$$

$$I_{qs\_B} = \sqrt{I_{s\max}^2 - \left(I_{ds\_B}\right)^2} \tag{25}$$

$$T_{\max}\left(\omega_e\right) = 3pL_m^2 I_{ds\_B} I_{qs\_B} \Big/ \left(2L_r\right) \tag{26}$$

3) THE CONSTANT VOLTAGE MODE ($\omega_1 < \omega_e$)

In the constant voltage mode, the diagram is shown in Fig.3 (c). When the excitation current and the torque current operates at the C point, the induction motor can output the maximum torque, where the C point is the only intersection of the voltage limit circle and the constant torque curve.

$$T_{\max}\left(\omega_e\right) = 3pL_m^2 I_{ds\_C} I_{qs\_C} \Big/ \left(2L_r\right) \tag{27}$$

$$\left(\omega_e \sigma L_s I_{ds\_C}\right)^2 + \left(\omega_e L_s I_{qs\_C}\right)^2 = V_{s\max}^2 \tag{28}$$

By combining the equations, the excitation current I_{ds_C}, the torque current I_{qs_C}, and the electromagnetic torque $T_{\max}\left(\omega_e\right)$ can be obtained for the C point, which are calculated as the equations (29)-(31).

$$T_{\max}\left(\omega_e\right) = 3pL_m^2 \left(\frac{V_{s\max}^2}{2\omega_e^2 \sigma L_s^2}\right) \Big/ 2L_r \tag{29}$$

$$I_{ds\_C} = V_{s\max} / \left(\sqrt{2}\omega_e L_s\right) \tag{30}$$

$$I_{qs\_C} = V_{s\max} / \left(\sqrt{2}\omega_e \sigma L_s\right) \tag{31}$$

IV. FIELD WEAKENING STRATEGY BASED ON CONSTRAINED MTPA CRITERION

The basic principle of field weakening strategy based on constrained MTPA criterion is to analytically solve the reference values of the excitation current and the torque current, with the minimum stator current as the optimization objective and at voltage and current limits, so as to realize the minimum stator current control strategy. In the electromagnetic torque equation (9), the values of the excitation current and the torque current are not unique, which is utilized to realize the MTPA control of induction motor. Under the same electromagnetic torque condition, MPTA control strategy can reduce the stator current amplitude, improve the efficiency of induction motor, and reduce the capacity of voltage source inverter. The solution of the reference values of stator current based on MTPA can be expressed as an optimization problem with nonlinear constraints, as shown in equations (32)-(36).

$$min\ I_s = \sqrt{\left(I_{ds}\right)^2 + \left(I_{qs}\right)^2} \tag{32}$$

$$s.t.\ \left(\omega_e \sigma L_s I_{qs}\right)^2 + \left(\omega_e L_s I_{ds}\right)^2 \le V_{s\max}^2 \tag{33}$$

$$\left(I_{ds}\right)^2 + \left(I_{qs}\right)^2 \le I_{s\max}^2 \tag{34}$$

$$\frac{3}{2} p \frac{L_m^2}{L_r} I_{ds} I_{qs} = T_e \tag{35}$$

$$T_e \le T_m\left(\omega_e\right) \tag{36}$$

The equation (32) is the objective function of the constrained optimization problem. In the steady state of the induction motor, the electromagnetic torque T_e can be expressed as the equation (35). The equation (36) expresses the maximum torque that the induction motor can output. The solution of the maximum torque T_m can be described as another optimization problem, which is shown as the equation (9)-(11). The above optimization problems can be solved analytically in the constant torque mode, the constant apparent power mode and the constant voltage mode.

A. THE CONSTANT TORQUE MODE ($0 < \omega_e \le \omega_{base}$)

The maximum torque $T_{\max}$ has been discussed, as shown in the equation (21). When the electromagnetic torque reference T_e is smaller than the maximum torque T_m in the constant torque mode, that is, $T_e < T_{\max}$, From Fig.4 (a), it can be seen that the intersection point D of the constant torque curve and the MTPA curve is closest to the dot, that is, the magnitude of the stator current corresponding to the D point is the smallest. Therefore, the excitation current I_{ds_D} and

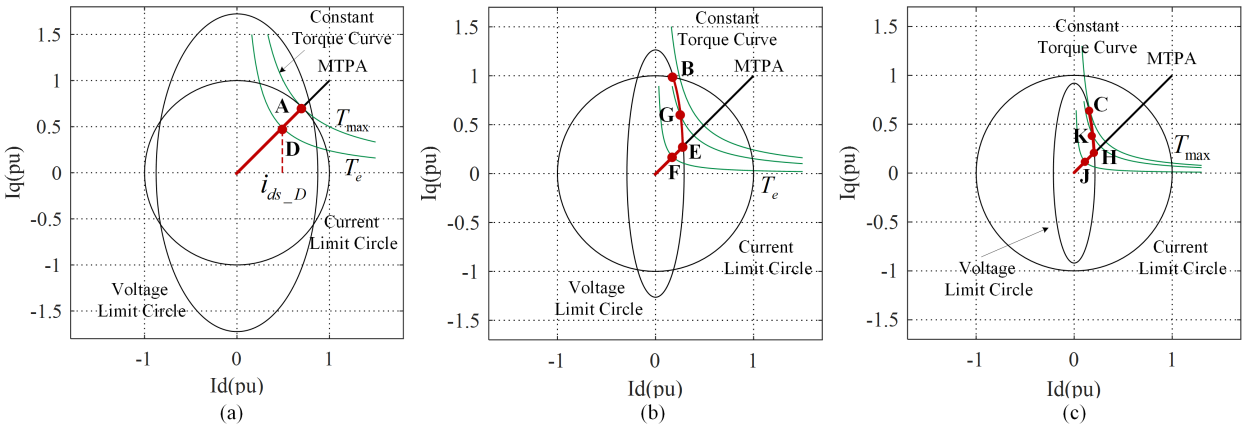

FIGURE 4. The diagram of optimal stator currents of field weakening based on MTPA.

the torque current I_{qs_D} corresponding to the D point are the reference values of the electromagnetic torque reference T_e. By combining the equations (37)-(38), the calculation equations of the excitation current and the torque current can be obtained as shown in the equation (39).

$$T_e = \frac{3}{2}p\frac{L_m^2}{L_r}I_{ds\_D}I_{qs\_D} \tag{37}$$

$$I_{ds\_D} = I_{qs\_D} \tag{38}$$

$$I_{ds\_D} = I_{qs\_D} = \sqrt{2T_eL_r \Big/ (3pL_m^2)} \tag{39}$$

B. THE CONSTANT APPARENT POWER MODE ($\omega_{base} < \omega_e \leq \omega_1$)

In the constant apparent power mode, voltage limit circle and current limit circle are shown in Fig.4 (b), where induction motor can output the maximum torque at the point B. The point E is the intersection of the voltage limit circle and the MTPA curve. The electromagnetic torque T_{e_E} corresponding to E can be obtained by combining the equations (40)-(41).

$$\left(\omega_e\sigma L_sI_{ds\_E}\right)^2 + \left(\omega_eL_sI_{qs\_E}\right)^2 = V_{s\max}^2 \tag{40}$$

$$I_{ds\_E} = I_{qs\_E} \tag{41}$$

When the electromagnetic torque reference T_e is less than the electromagnetic torque T_{e_E} corresponding to E, on the constant torque curve, the intersection point F of the constant torque curve and the MTPA curve is closest to the dot, that is, the magnitude of the stator current corresponding to the F point is the smallest. By combining the equations (42)-(43), the calculation equations of the excitation current and the torque current corresponding to the point F can be obtained, as shown in the equation (44).

$$T_e = \frac{3}{2}p\frac{L_m^2}{L_r}I_{ds\_F}I_{qs\_F} \tag{42}$$

$$I_{ds\_F} = I_{qs\_F} \tag{43}$$

$$I_{ds\_F} = I_{qs\_F} = \sqrt{2T_eL_r \Big/ (3pL_m^2)} \tag{44}$$

When $T_{e\_E} < T_e < T_{\max}$, it can be seen that, from Fig.4 (c), in the constant torque curve, the intersection G of the constant torque curve and the voltage limit circle is closest to the dot. Therefore, the excitation current I_{ds_G} and the torque current I_{qs_G} for the G point are stator current references of T_e based on MTPA control strategy. I_{ds_G} and I_{qs_G} can be obtained by combining the equations (45)-(46).

$$T_e = \frac{3}{2}p\frac{L_m^2}{L_r}I_{ds\_G}I_{qs\_G} \tag{45}$$

$$\left(\omega_e\sigma L_sI_{ds\_G}\right)^2 + \left(\omega_eL_sI_{qs\_G}\right)^2 = V_{s\max}^2 \tag{46}$$

C. THE CONSTANT VOLTAGE ($\omega_1 < \omega_e$)

In the constant voltage mode, voltage limit circle and current limit circle are shown in Fig.4 (c), where induction motor can output the maximum torque at the point C in the constant voltage mode. The point H is the intersection of the voltage limit circle and the MTPA curve. The electromagnetic torque T_{e_H} corresponding to H can be obtained by combining the equations (47)-(48).

$$\left(\omega_e\sigma L_sI_{ds\_H}\right)^2 + \left(\omega_eL_sI_{qs\_H}\right)^2 = V_{s\max}^2 \tag{47}$$

$$I_{ds\_H} = I_{qs\_H} \tag{48}$$

When $T_e < T_{e\_H}$, from Fig.4 (c), it can be seen that, on the constant torque curve, the point J of the constant torque curve and the MTPA curve is closest to the dot, that is, the magnitude of the stator current of the point J is the smallest.

Therefore, the excitation current I_{ds_J} and the torque current I_{qs_J} corresponding to the point J are the references of T_e based on MTPA. By combining the equations (49)-(50), the calculation equations of I_{ds_J} and I_{qs_J} can be obtained as shown in the equation (51).

$$T_e = \frac{3}{2}p\frac{L_m^2}{L_r}I_{ds\_F}I_{qs\_F} \tag{49}$$

$$I_{ds\_J} = I_{qs\_J} \tag{50}$$

$$I_{ds\_J} = I_{qs\_J} = \sqrt{2T_eL_r \Big/ (3pL_m^2)} \tag{51}$$

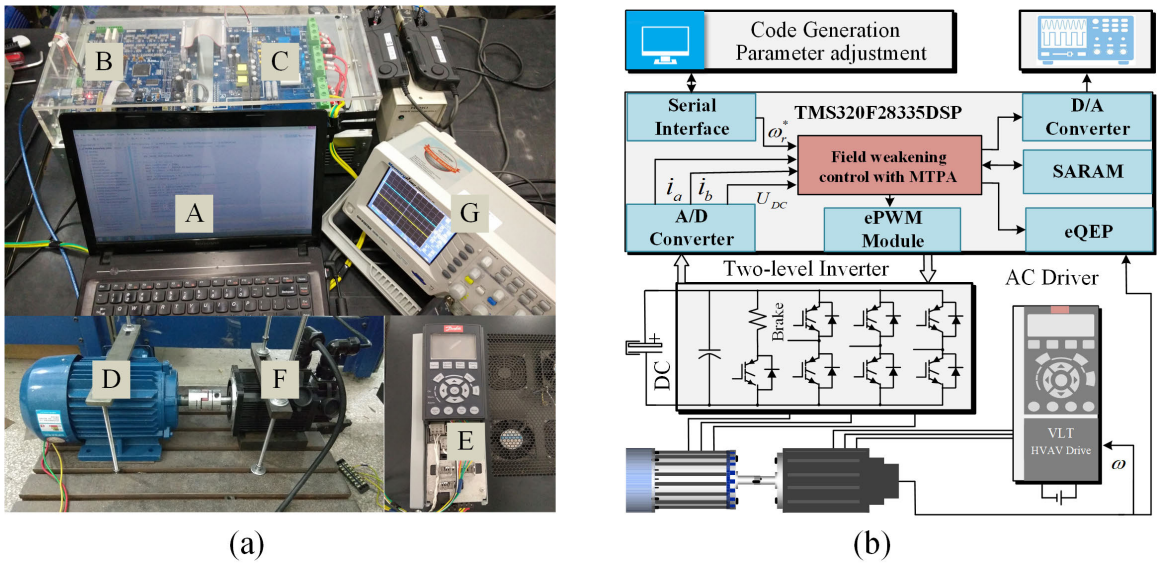

FIGURE 5. (a) Block diagram of the experimental platform:(A) the computer (B) TMS320F28335 DSP (C) VSI (D) induction machine (E) Danfoss frequency converter (F) SPMSM; (b) the control block diagram of experimental platform.

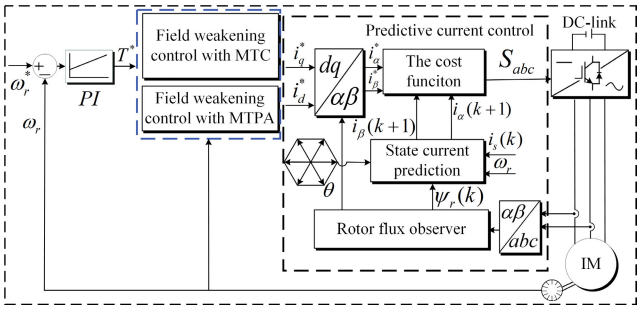

FIGURE 6. Block diagram of the proposed field weakening based on MTPA.

When $T_{e\_H} < T_e < T_{\max}$, from Fig.4 (c), it can be seen that, in constant torque curve, the intersection K of the constant torque curve and the voltage limit circle is closest to the dot. I_{ds_K} and I_{qs_K} can be obtained by combining the equations (52)-(53).

$$T_e = \frac{3}{2} p \frac{L_m^2}{L_r} I_{ds\_K} I_{qs\_K} \tag{52}$$

$$\left(\omega_e \sigma L_s I_{ds\_K}\right)^2 + \left(\omega_e L_s I_{qs\_K}\right)^2 = V_{s\max}^2 \tag{53}$$

V. EXPERIMENTAL EVALUATION

The experimental platform is presented in Fig.5, where induction machine is fed by voltage source inverter and digital signal processor (TMS320F28335 DSP). The functions of each module of digital signal processor are shown in Fig.6, which includes A/D conversion, rotor position acquisition, PWM output, D/A conversion and communication. Permanent magnet synchronous motor and frequency converter constitute the load system to provide load torque. The proposed algorithm is implemented with C code using Code Composer Studio 3.3 of Texas Instruments. Main frequency

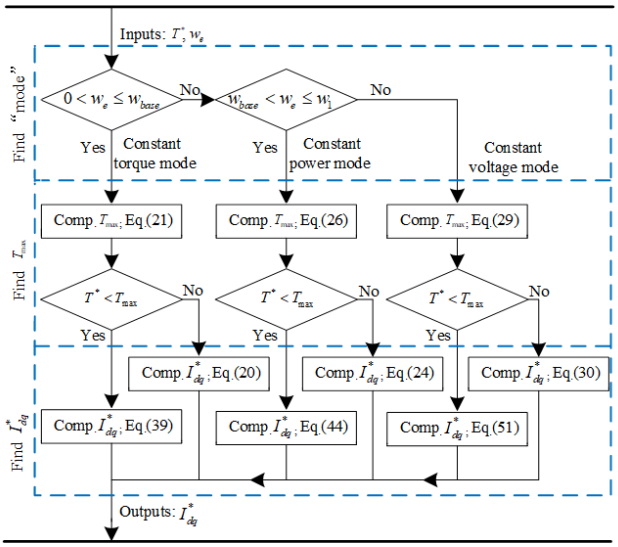

FIGURE 7. Calculation of references of excitation current and torque current.

of TMS320F28335 DSP is 150MHz. The references of stator currents are obtained according to Fig.7.

The diagram of induction machine control system is shown in Fig.6. The electromagnetic torque reference of induction motor is derived from the proportional-integral regulator of the speed loop. The calculation of stator excitation current reference and torque current reference can be divided into two methods, field weakening control based on MTC, and field weakening control based on MTPA. The predictive current control is used to track the stator current references.

The dynamic performance for field weakening based on MTPA is shown in Fig.8. The speed command changes from 4000 r/min to -4000 r/min, and then back to 4000 r/min.

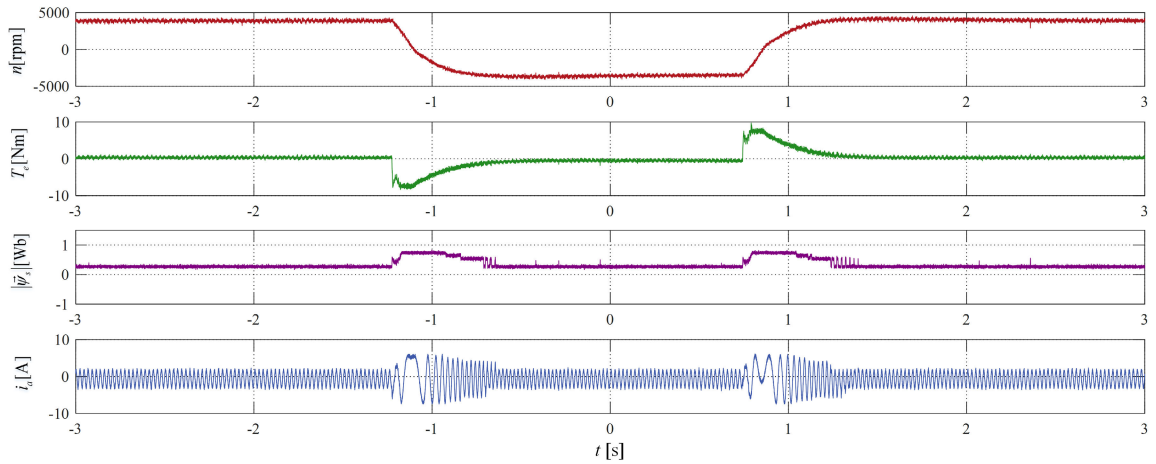

FIGURE 8. The dynamic performance for field weakening based on MTPA.

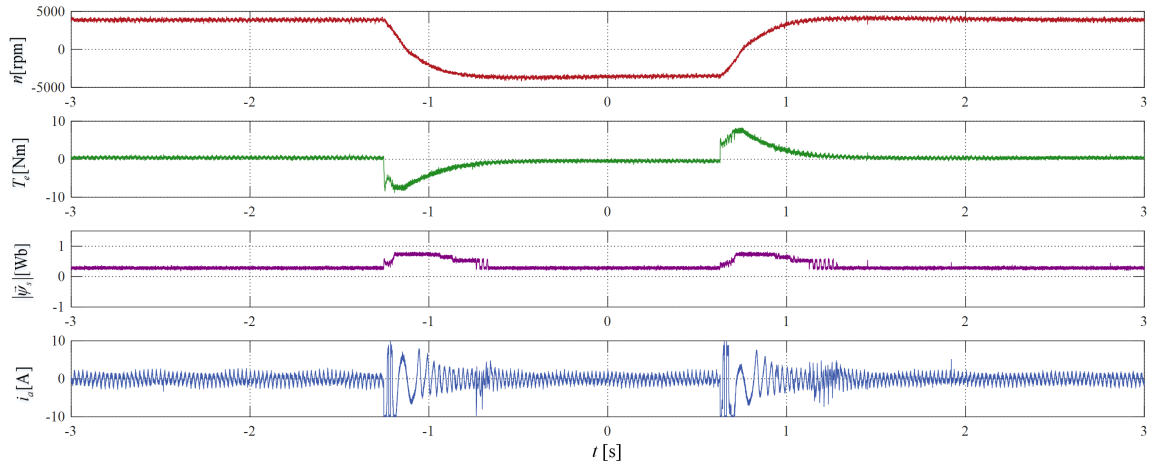

FIGURE 9. The dynamic performance for field weakening based on MTPA with mismatched parameter $\hat{L}_m = 0.5L_m$.

TABLE 1. Parameters of induction machine.

Descriptions	Parameters	Nominal Values
DC-link Voltage	$V_{dc}\,[V]$	582
Rated Frequency	$f_N\,[Hz]$	50
Rated Speed	$\omega_{nom}\,[r/min]$	2772
Number of Pole Pairs	p	1.0
Stator Resistance	$R_s\,[\Omega]$	2.68
Rotor Resistance	$R_r\,[\Omega]$	2.13
Mutual Inductance	$L_m\,[H]$	0.275
Stator Inductance	$L_s\,[H]$	0.283
Rotor Inductance	$L_r\,[H]$	0.283
Inertia of IM	$J_{nom}\,[kg \cdot m^2]$	0.005
Flux Reference	$\lvert\boldsymbol{\psi_s}\rvert^*[Wb]$	0.71

It can be seen that the stator flux amplitude in steady state is less than that in dynamic state, because in steady state, the excitation current and torque current are calculated based on MTPA. The dynamic performance for field weakening based on MTPA with mismatched parameter $\hat{L}_m = 0.5L_m$ is presented in Fig.9, where $\hat{L}_m$ denotes the mismatched parameter and L_m is the nominal parameter. It can be seen

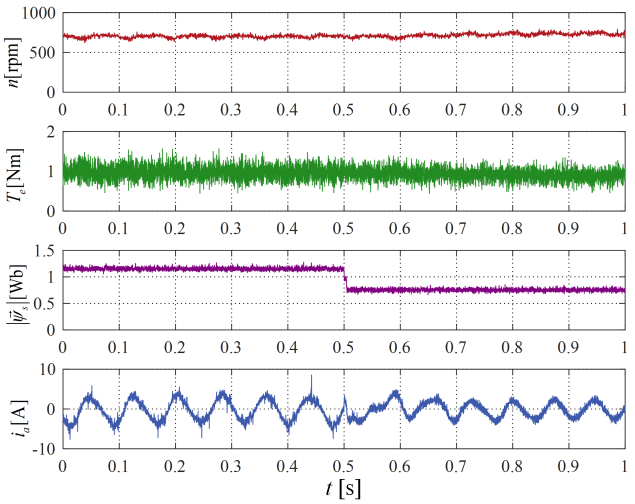

FIGURE 10. The field weakening control based on MTC is switched to that of MTPA at 0.5 *s* when the speed is 750 *r* / min and the load torque is 1.0 *Nm*.

that MTPA with mismatched parameter can lead to large electromagnetic torque ripple and stator current harmonic content.

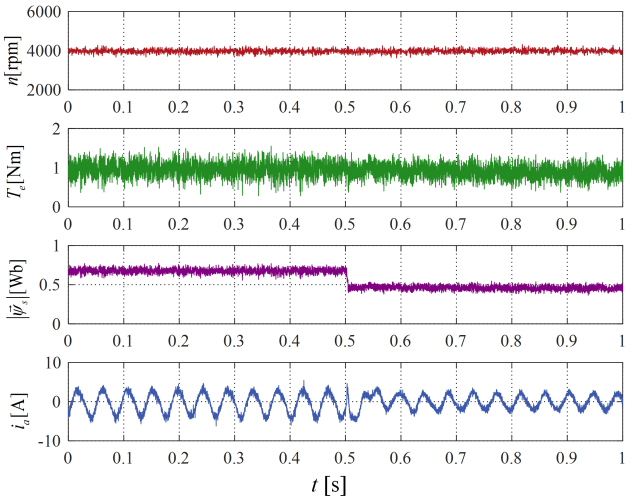

FIGURE 11. The field weakening control based on MTC is switched to that of MTPA at 0.5 *s* when the speed is 4000 *r* / min and the load torque is 1.0 *Nm*.

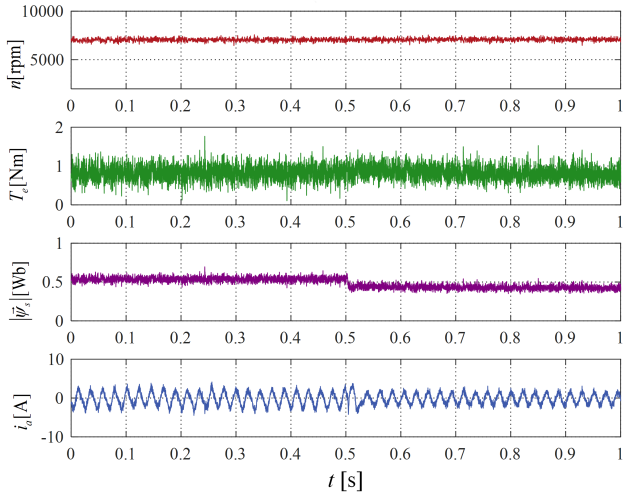

FIGURE 12. The field weakening control based on MTC is switched to that of MTPA at 0.5 *s* when the speed is 7500 *r* / min and the load torque is 1.0 *Nm*.

In order to verify the influence of MTC and MTPA on the stator flux and stator current amplitude, the switching Experiments of two Control Strategies are carries out under three conditions: the speed 750 r/min and load torque 1.0 Nm, the speed 4000 r/min and load torque 1.0 Nm, the speed 7500 r/min and load torque 1.0 Nm. The experimental results are shown in Fig.10-Fig.12. It can be seen that when the induction motor is switched from MTC to MTPA at 0.5 s, the stator flux amplitude decreases and the stator current amplitude becomes smaller.

In order to compare MTC and MTPA in detail, the comparative experiments are carried out under the conditions of the speed 500 r/min and the load torque 0.375 Nm, 1.5 Nm, 3.75 Nm, 5.625 Nm, 7.5 Nm, the speed 4000 r/min and the load torque 0.375 Nm, 1.5 Nm, 3.75 Nm. At steady state, the experiment results are shown in Table 2. Compared with MTC, MTPA reduces the stator current amplitude.

TABLE 2. Stator current references based on MTC and MTPA at $n = 500r/\min$.

T_L/Nm	0.375	1.5	3.75	5.625	7.5
MTC_I_d/A	4.63	4.65	4.62	4.66	4.65
MTC_I_q/A	0.31	0.81	2.05	3.05	4.05
$MTPA\_I_d/A$	1.02	2.03	3.12	3.83	4.32
$MTPA\_I_q/A$	1.05	2.13	3.13	3.85	4.33
MTC_I_s/A	4.64	4.72	5.05	5.57	6.16
$MTPA\_I_s/A$	1.46	2.94	4.42	5.43	6.11

TABLE 3. Stator current references based on MTC and MTPA at $n = 4000r/\min$.

T_L/Nm	0.375	1.5	3.75
MTC_I_d/A	2.62	2.65	2.67
MTC_I_q/A	0.37	1.51	3.59
$MTPA\_I_d/A$	0.98	1.96	2.64
$MTPA\_I_q/A$	1.05	2.03	3.51
MTC_I_s/A	2.65	3.05	4.47
$MTPA\_I_s/A$	1.44	2.82	4.39

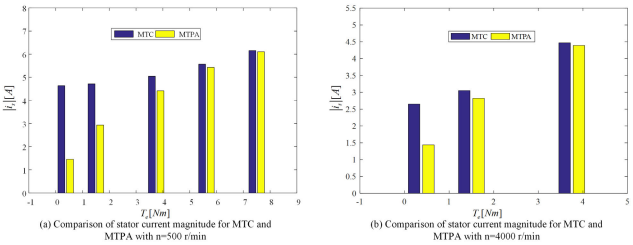

FIGURE 13. Comparison of stator current magnitude for MTC and MTPA.

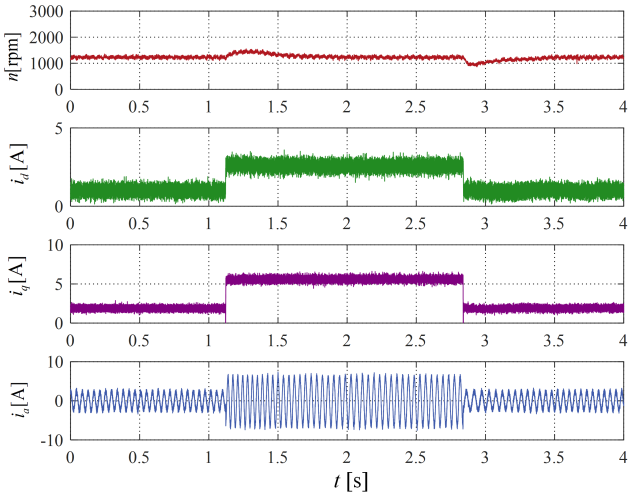

FIGURE 14. Model predictive current control of induction motor.

In order to verify predictive current control for stator current tracking strategy, stator excitation current reference changes from 1.0 A to 3.0 A at 1.15 s, and from 3.0 A to 1.0 A at 2.85 s. Stator torque current reference changes from 2.0 A to 5.0 A at 1.15 s, and from 5.0 A to 2.0 A at 2.85 s. The experimental results are shown in Fig.14. It can be seen that stator current has a fast dynamic response. Fig.14 (b) is the transient response for stator excitation current and torque

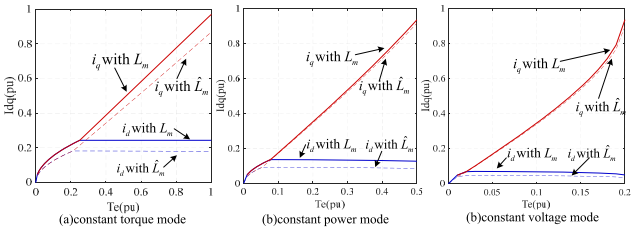

FIGURE 15. The influence of mismatched parameter on stator current reference computation.

current. For predictive current control, the response time of stator current is only 0.6 *ms*.

The influence of mismatched parameter $\hat{L}_m$ on computation of excitation current and torque current references is presented in Fig.15, where $\hat{L}_m = 0.5L_m$. It can be seen that as the speed increases, the influence of $\hat{L}_m$ reduces.

VI. CONCLUSION

In this paper, the constrained MTPA control for induction machine drives is proposed. Firstly, this paper establishes a nonlinear optimization problem at voltage and current limits, where the objective of this optimization problem is to minimize the stator current. Secondly, the principle of sub-mode is proposed to analytically obtain the expressions of stator excitation current and torque current references. Finally, the experimental results verify the effectiveness of the proposed method. However, the method proposed in this paper depends on the parameters of induction motor, which will affect the accuracy of stator current references. The MTPA control based on parameter identification will be the direction of further research.

REFERENCES

[1] K. Li and Y. Wang, "Maximum torque per ampere (MTPA) control for IPMSM drives based on a variable-equivalent-parameter MTPA control law," *IEEE Trans. Power Electron.*, vol. 34, no. 7, pp. 7092–7102, Jul. 2019.

[2] Q. Chen, W. Zhao, G. Liu, and Z. Lin, "Extension of virtual-signal-injection-based MTPA control for five-phase IPMSM into fault-tolerant operation," *IEEE Trans. Ind. Electron.*, vol. 66, no. 2, pp. 944–955, Feb. 2019.

[3] T. Sun, J. Wang, and M. Koc, "On accuracy of virtual signal injection based MTPA operation of interior permanent magnet synchronous machine drives," *IEEE Trans. Power Electron.*, vol. 32, no. 9, pp. 7405–7408, Sep. 2017.

[4] N. Bedetti, S. Calligaro, C. Olsen, and R. Petrella, "Automatic MTPA tracking in IPMSM drives: Loop dynamics, design, and auto-tuning," *IEEE Trans. Ind. Appl.*, vol. 53, no. 5, pp. 4547–4558, Sep. 2017.

[5] X. Zhou, Y. Zhou, H. Wang, M. Lu, F. Zeng, and Y. Yu, "An improved MTPA control based on amplitude-adjustable square wave injection," *IEEE Trans. Energy Convers.*, vol. 35, no. 2, pp. 956–965, Jun. 2020.

[6] A. Yoo, S.-K. Sul, H. Kim, and K.-S. Kim, "Flux-weakening strategy of an induction machine driven by an electrolytic-capacitor-less inverter," *IEEE Trans. Ind. Appl.*, vol. 47, no. 3, pp. 1328–1336, May 2011.

[7] S.-H. Kim and S.-K. Sul, "Voltage control strategy for maximum torque operation of an induction machine in the field-weakening region," *IEEE Trans. Ind. Electron.*, vol. 44, no. 4, pp. 512–518, Aug. 1997.

[8] J. Su, R. Gao, and I. Husain, "Model predictive control based field-weakening strategy for traction EV used induction motor," *IEEE Trans. Ind. Appl.*, vol. 54, no. 3, pp. 2295–2305, May 2018.

[9] X. Zhang, B. Wang, Y. Yu, J. Zhang, J. Dong, and D. Xu, "Analysis and optimization of current dynamic control in induction motor field-weakening region," *IEEE Trans. Power Electron.*, vol. 35, no. 9, pp. 8860–8866, Sep. 2020.

[10] S. K. Sahoo and T. Bhattacharya, "Field weakening strategy for a vector-controlled induction motor drive near the six-step mode of operation," *IEEE Trans. Power Electron.*, vol. 31, no. 4, pp. 3043–3051, Apr. 2016.

[11] A. A. Ahmed, B. K. Koh, and Y. I. Lee, "A comparison of finite control set and continuous control set model predictive control schemes for speed control of induction motors," *IEEE Trans. Ind. Informat.*, vol. 14, no. 4, pp. 1334–1346, Apr. 2018.

[12] S. K. Sahoo and T. Bhattacharya, "Field weakening strategy for a vector-controlled induction motor drive near the six-step mode of operation," *IEEE Trans. Power Electron.*, vol. 31, no. 4, pp. 3043–3051, Apr. 2016.

[13] T. Deng, Z. Su, J. Li, P. Tang, X. Chen, and P. Liu, "Advanced angle field weakening control strategy of permanent magnet synchronous motor," *IEEE Trans. Veh. Technol.*, vol. 68, no. 4, pp. 3424–3435, Apr. 2019.

[14] N. Zhao and N. Schofield, "Field-weakening capability of interior permanent-magnet machines with salient pole shoe rotors," *IEEE Trans. Magn.*, vol. 53, no. 11, pp. 1–7, Nov. 2017.

[15] J. Su, R. Gao, and I. Husain, "Model predictive control based field-weakening strategy for traction EV used induction motor," *IEEE Trans. Ind. Appl.*, vol. 54, no. 3, pp. 2295–2305, May 2018.

[16] S.-Y. Jung, C. Chris Mi, and K. Nam, "Torque control of IPMSM in the field-weakening region with improved DC-link voltage utilization," *IEEE Trans. Ind. Electron.*, vol. 62, no. 6, pp. 3380–3387, Jun. 2015.

[17] Y. Zhang, Y. Bai, H. Yang, and B. Zhang, "Low switching frequency model predictive control of three-level inverter-fed IM drives with speed-sensorless and field-weakening operations," *IEEE Trans. Ind. Electron.*, vol. 66, no. 6, pp. 4262–4272, Jun. 2019.

[18] S. Kim and J.-K. Seok, "Finite-settling-steps direct torque and flux control for torque-controlled interior PM motors at voltage limits," *IEEE Trans. Ind. Appl.*, vol. 50, no. 5, pp. 3374–3381, Sep. 2014.

[19] S. K. Sahoo and T. Bhattacharya, "Field weakening strategy for a vector-controlled induction motor drive near the six-step mode of operation," *IEEE Trans. Power Electron.*, vol. 31, no. 4, pp. 3043–3051, Apr. 2016.

[20] M. Mengoni, L. Zarri, A. Tani, G. Serra, and D. Casadei, "A comparison of four robust control schemes for field-weakening operation of induction motors," *IEEE Trans. Power Electron.*, vol. 27, no. 1, pp. 307–320, Jan. 2012.

[21] J. Su, R. Gao, and I. Husain, "Model predictive control based field-weakening strategy for traction EV used induction motor," *IEEE Trans. Ind. Appl.*, vol. 54, no. 3, pp. 2295–2305, May 2018.

[22] S. Bozhko, S. Dymko, S. Kovbasa, and S. M. Peresada, "Maximum torque-per-amp control for traction IM drives: Theory and experimental results," *IEEE Trans. Ind. Appl.*, vol. 53, no. 1, pp. 181–193, Jan. 2017.

[23] W. Sung, J. Shin, and Y.-S. Jeong, "Energy-efficient and robust control for high-performance induction motor drive with an application in electric vehicles," *IEEE Trans. Veh. Technol.*, vol. 61, no. 8, pp. 3394–3405, Oct. 2012.

[24] J.-K. Seok and S.-K. Sul, "Optimal flux selection of an induction machine for maximum torque operation in flux-weakening region," *IEEE Trans. Power Electron.*, vol. 14, no. 4, pp. 700–708, Jul. 1999.

[25] D.-C. Lee, S.-K. Sul, and M.-H. Park, "High performance current regulator for a field-oriented controlled induction motor drive," *IEEE Trans. Ind. Appl.*, vol. 30, no. 5, pp. 1247–1257, Sep. 1994.

[26] S.-H. Kim and S.-K. Sul, "Voltage control strategy for maximum torque operation of an induction machine in the field-weakening region," *IEEE Trans. Ind. Electron.*, vol. 44, no. 4, pp. 512–518, Aug. 1997.

ZHIHUA PENG was born in Hunan, China, in 1986. He received the B.S. degree in electrical engineering from Jilin Engineering Normal University, Changchun, China, in 2011, and the M.S. degree in electric machine and electric apparatus from the Shenyang University of Technology, Shenyang, China, in 2014. He joined the Motor Department, Midea Group, in April 2014, where he engaged in the research of permanent magnet synchronous motor. Since August 2015, he has been working with the School of Electrical Engineering, Shaoyang University. His research interests include permanent magnet synchronous motor design and model predictive control.